JGR Biogeosciences

RESEARCH ARTICLE
10.1029/2019JG005222

Key Points:
- The main factors that influenced wetland greenhouse gas emissions were plant growth, water flow, and nitrogen loading
- The restored wetland was a much stronger carbon sink than the natural wetland by maximizing CO_2 uptake and minimizing CH_4 emissions
- Altering species composition and water flow as part of wetland restoration was an innovative strategy for mitigating climate change

Supporting Information:
- Supporting Information S1

Correspondence to:
J. Tang and X. Chen,
jimtang1999@gmail.com;
xcchen@des.ecnu.edu.cn

Citation:
Yang, H., Tang, J., Zhang, C., Dai, Y., Zhou, C., Xu, P., et al. (2020). Enhanced carbon uptake and reduced methane emissions in a newly restored wetland. *Journal of Geophysical Research: Biogeosciences*, *125*, e2019JG005222. https://doi.org/10.1029/2019JG005222

Received 10 MAY 2019
Accepted 19 DEC 2019
Accepted article online 4 JAN 2020

Corrected 9 FEB 2020
This article was corrected on 7 FEB 2020. See the end of the full text for details.

Enhanced Carbon Uptake and Reduced Methane Emissions in a Newly Restored Wetland

Hualei Yang[1], Jianwu Tang[1,2], Chunsong Zhang[1], Yuhang Dai[1], Cheng Zhou[1], Ping Xu[1], Danielle C. Perry[3], and Xuechu Chen[1]

[1]State Key Laboratory of Estuarine and Coastal Research, Shanghai Key Lab for Urban Ecological Processes and Eco-Restoration, School of Ecological and Environmental Sciences, Institute of Eco-Chongming, East China Normal University, Shanghai, China, [2]The Ecosystems Center, Marine Biological Laboratory, Woods Hole, MA, USA, [3]College of the Environment and Life Sciences, University of Rhode Island, Kingston, RI, USA

Abstract Wetlands play an important role in reducing global warming potential in response to global climate change. Unfortunately, due to the effects of human disturbance and natural erosion, wetlands are facing global extinction. It is essential to implement engineering measures to restore damaged wetlands. However, the carbon sink capacity of restored wetlands is unclear. We examined the seasonal change of greenhouse gas emissions in both restored wetland and natural wetland and then evaluated the carbon sequestration capacity of the restored wetland. We found that (1) the carbon sink capacity of the restored wetland showed clear daily and seasonal change, which was affected by light intensity, air temperature, and vegetation growth, and (2) the annual daytime (8–18 hr) sustained-flux global warming potential was -11.23 ± 4.34 kg CO_2 m^{-2} y^{-1}, representing a much larger carbon sink than natural wetland (-5.04 ± 3.73 kg CO_2 m^{-2} y^{-1}) from April to December. In addition, the results showed that appropriate tidal flow management may help to reduce CH_4 emission in wetland restoration. Thus, we proposed that the restored coastal wetland, via effective engineering measures, reliably acted as a large net carbon sink and has the potential to help mitigate climate change.

1. Introduction

Currently, substantial greenhouse gas (GHG) emissions, including carbon dioxide (CO_2), methane (CH_4), and nitrous oxide (N_2O), have contributed to global climate change, which is a threat to human survival and development (Intergovernmental Panel on Climate Change, 2014). It is urgently needed to explore more approaches to fix carbon and reduce GHG emissions to mitigate climate change progression (National Academy of Sciences, 2018).

Coastal wetlands (e.g., salt marshes), the ecological buffer zones between the land and ocean, are large soil carbon stocks that can maintain rapid carbon sequestration (therefore significant blue carbon ecosystems) with high photosynthetic capacity and low decomposition rates (Tang et al., 2018). Compared to terrestrial carbon sinks (e.g., forests), blue carbon ecosystems sequester 10 times or more carbon than terrestrial ecosystems due to the long-term storage of carbon in sediments (Mcleod et al., 2011). Therefore, protecting and maintaining vulnerable but important wetland carbon stocks to avoid emissions and the release of stored carbon are important approaches for climate change mitigation efforts.

Natural wetlands have shown tolerance when confronted with human impacts and climate change effects (Kirwan et al., 2016; Kirwan & Megonigal, 2013). However, in some severely damaged wetlands, vulnerability to environmental stressors is high and the effects may be irreversible. These large-scale coastal wetlands and their associated ecosystem services have declined due to the combined effects of human disturbance and natural erosion (Mitsch & Gosselink, 2000).

Previously, coastal wetland restoration implementations mainly focused on restoring tidal marshes by introducing tidal flow, amending sediment, and transplanting plants (Mitsch & Gosselink, 2000). Recently, as blue carbon has attracted global attention (supporting information, Table S1), coastal wetland restoration projects are expected to incorporate methods to enhance carbon sequestration that go beyond just restoring marshes (Mander et al., 2015; Zhou et al., 2016). Unfortunately, up until now, most researchers focused on the water quality and biodiversity and rarely quantified blue carbon potential of restored wetlands. Nevertheless, most blue carbon studies on coastal wetlands mainly focused on CO_2 sequestration and often ignored CH_4 and N_2O emissions (Kroeger et al., 2017). CH_4 and N_2O have larger global warming potentials per molecule, about 25 and 298 times higher than that of CO_2, respectively (Brannon et al., 2016). Thus, if the restored wetland increases CH_4 or N_2O emissions, it alters the overall benefit of CO_2 sequestration (García-Lledó et al., 2011; Rosentreter et al., 2018).

In this study, in situ GHG measurements (CO_2, CH_4, and N_2O) were simultaneously collected in the field to accurately estimate the blue carbon storage of the whole ecosystem in the coastal restored and natural wetlands, which may be offset by CH_4 and N_2O emissions. The aim is to discuss the global warming potential and accurately assess the ecosystem carbon service (CO_2 uptake capacity and CH_4 emissions) of the restored wetland via effective engineering measures. The results will lead to a greater understanding of blue carbon ecology and promote the implementation of wetland restoration worldwide.

2. Materials and Methods

2.1. Study Sites

This study was conducted within the coastal wetlands of northern Hangzhou Bay, Shanghai, China. The Yingwuzhou wetland (restored wetland) and the Fengxian wetland (natural wetland) were used to explore the blue carbon effect of the restored wetland throughout the year of 2018. These two study sites were 20 km apart (Figure S1). The Yingwuzhou wetland and the Fengxian wetland cover an area of 23 and 8,000 ha, respectively, and are representative of the restored and natural estuarine wetlands in southeast China.

Yingwuzhou wetland, located in Jinshan District in Shanghai, China (N30°42′26.73″, E121°20′04.15″), was restored in 2016 by amending the sediment, constructing an ecological dam to prevent erosion, and transplanting local plants. This restored wetland provided ecological benefits of water quality improvement and biodiversity protection. Before restoration, the Yingwuzhou wetland was a *Phragmites australis* and *Spartina alterniflora* dominated wetland, like the Fengxian natural wetland. To protect the native species —*Phragmites australis*, as one of the major goals of the wetland restoration in Shanghai, we just transplanted *Phragmites australis* but not *Spartina alterniflora* in Yingwuzhou wetland. The salinity and pH of the wetland water were 10 ± 1.22‰ and 6.40 ± 0.13, respectively. A culvert was designed to connect the inside wetland and outside tidal water. Consequently, though there is no tidal flooding, we could control water exchange and maintain a desired water level by controlling the valve of the culvert (Figure S2).

The natural wetland site is located in Fengxian District, Shanghai (N30°50′33.75″, E121°39′03.60″). The dominant species are *Phragmites australis* and *Spartina alterniflora* in this area, which were flooded by high tide on the first and 15th of every lunar month. The salinity and pH of the wetland water were 19.28 ± 2.12‰ and 6.45 ± 0.12, respectively.

2.2. GHG Flux Measurements

At the restored and natural wetland site, five plots (2×2 m, the plots were 8 m apart from each other) were installed at each site during the winter of 2017. Within each plot, three PVC rings (20-cm height × 20-cm diameter, and installed into the soil to a depth of 10 cm) were placed, which represented the three replicates per plot that were established in both the restored and natural wetlands.

CO_2 and CH_4 fluxes were measured simultaneously in situ throughout the year of 2018, using an Ultra-Portable GHG Analyzer (Los Gatos Inc., CA, USA). A 2-m-high, 0.2-m-diameter transparent polycarbonate chamber was used to accommodate the height of the plants (up to 2 m) inside the chamber, with a mini-fan inside the chamber to ensure air circulation during measurements. Nylon tubing (0.46-cm inner diameter and approximately 10 m in total length) was connected to the analyzer via two gastight ports in a closed loop. Gas measurements were conducted for 5–10 min per plot, based on observed periods for linear rates of change. Before the GHG measurements, we made modifications to the instrument and kept the static transparent chamber be gastight in order to accomplish a closed-loop static flux chamber.

The N_2O concentration measurement was performed by adopting a closed static chamber-gas chromatograph technique (Brannon et al., 2016). The gas samples were drawn from the static transparent chamber into 60-ml nylon syringe at 0, 5, 10, 15, and 20 min and then transferred to the 50-ml vacuum airbag (MBT41-0.1, Haide Technologies Co. Ltd., Dalian, China; Brannon et al., 2016). The concentration of N_2O was measured by the gas chromatograph (7890A, Agilent Technologies Co. Ltd., CA, USA) with the electronic capture detector. The column temperature and the detector temperature were set as 60 and 330 °C, respectively, and the carrier gas flow rate was 10 ml min^{-1}.

To draw monthly comparisons of the restored and natural wetlands at similar environmental conditions (e.g., light intensity, temperature, and plant phenology), all GHG flux measurements were performed between 10:00 and 15:00 on clear, sunny days to quantify the random error (i.e., daily difference; Lavoie et al., 2014). There was a minimal monitoring interval between the two sites (usually, measurements were finished within 2 days, unless there was inclement weather).

2.3. GHG Fluxes and Sustained-Flux Global Warming Potential Calculations

GHG fluxes were calculated using the linear change in gas concentrations over time with field-measured air temperatures and atmospheric pressure (Martin & Moseman-Valtierra, 2017) during the measurement period, following the formula:

$$F = \frac{dC}{dt} \times \frac{PV}{RAT}, \tag{1}$$

where F is the GHG flux (μmol m^{-2} s^{-1}); dC/dt is the changing concentration over time (μmol mol^{-1}); P is the air pressure, standard is 101,223.7 (Pa); V is the effective volume of the static closed chamber (m^3); R is the gas constant, defaulted to 8.3144 (J mol K); A is the base area of the chamber (m^2); and T is the air temperature (K). For CO_2/CH_4 data analysis, the first 30 s and the end 30 s of measurements were not included in the flux calculations to account for gases passing through the length of the tubing between the analyzer and the chamber. When dC/dt had an R^2 value of less than 0.9 and p value greater than 0.05, data were not included in the analysis.

Radiative forcing (W m^{-2}) is a useful measurement to estimate the potential climatic effect induced by the changing concentrations of radiatively active (greenhouse) gases, solar radiation, aerosols, and albedo (Boucher & Haywood, 2001; Frolking et al., 2006; Jain et al., 2000). In this study, we used sustained-flux global warming potential (SGWP) to estimate the dynamics of total radiative forcing as ecosystem GHG fluxes are sustained ones. SGWP was calculated with scalers of 45 for CH_4 and 270 for N_2O considering the warming effect over the 100-year period (Neubauer & Megonigal, 2015). Because of lack of nighttime flux measurement, here we only calculate daytime (8–18 hr) SGWP scaled to a day or a year. In addition, we estimated the annual average SGWP from April to December in the restored and natural wetlands.

$$\mathrm{SGWP} = F\mathrm{CO_2} + (F\mathrm{CH_4} \times 45) + (F\mathrm{N_2O} \times 270). \tag{2}$$

where FCO_2, FCH_4, FN_2O are mass flux in units (for example, μg CO_2 m^{-2} s^{-1}).

2.4. Plant Physiological Properties

To obtain the plants' chlorophyll concentration measurement, we used a Soil Plant Analysis Development-502 meter. This equipment is widely used as a nondestructive, inexpensive, rapid, and accurate tool that utilizes leaf transmittance in two wavebands centered at 650 and 940 nm (Yang et al., 2017). We selected five leaves per plot (25 leaves per site). For each leaf, we made five Soil Plant Analysis Development readings, which were evenly distributed over the entire leaf area and then averaged.

In the summer, we investigated the plant biomass (the live vegetation biomass per unit area) in the restored and natural wetlands. In each site, we randomly set seven quadrats (1 × 1 m) near the plots and cut the vegetation (aboveground biomass) in the quadrats. Then the vegetation was taken back to the lab and dried in the oven (65 °C) for at least 48 hr to quantify leaf dry mass.

2.5. Key Environmental Parameters

The environmental data were obtained from the Micro Weather Station (Onset-U30, USA). The data logger collected the following measurements every 5 min: photosynthetically active radiation (μmol m^{-2} s^{-1}), air temperature (T_{air}, °C), relative humidity (%), and so forth. Soil pH, oxidation-reduction potential (ORP), temperature, moisture, and water salinity point measurements were performed monthly in each PVC ring. Soil ORP and pH were measured using an ORP meter (FJA-6, Nanjing, China), soil temperature and moisture were measured by Decagon EC-5 sensors (Decagon Devices, Pullman, WA, USA), and water salinity was

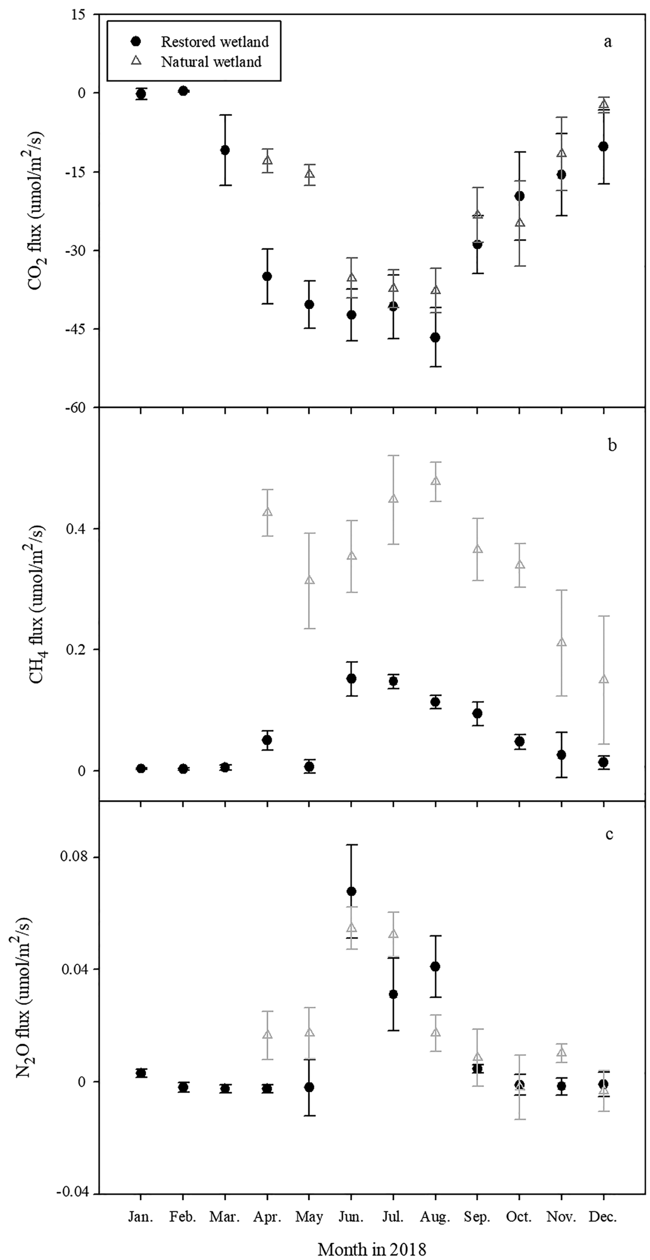

Figure 1. The seasonal variations of GHG emissions (mean ± SD) in the restored and natural wetlands.

measured by a handheld refractometer (MASTER-S/Millα, ATAGO, Japan) by applying water extracted from approximately 5 ml of surface soil.

The soil samples used to obtain soil organic carbon (SOC) were collected from the cores centered at 15-cm depth in August. Three soil subsamples were randomly collected and then mixed as one sample in each PVC ring. After collection, we separated undecomposed dead plant matter from the samples and placed the samples in a cooler and taken back to the lab. After they were dried and ground into powder, the soil samples were filtered through a 150-μm mesh screen. The soil samples were acidified with 1 mol L^{-1} of HCl to remove the inorganic carbon (Vuong et al., 2013). Then, the samples were ground again, and 2 mg of the sample was used for SOC determination by an Elemental Analyzer (Vario MICRO cube, Elementar, Germany).

For the dissolved inorganic nitrogen (DIN) analysis, the Rhizon soil moisture samplers (Rhizophere Research Products, Wageningen, Netherlands) were used to sample the pore water (50 ml in each plot) within a 15- to 20-cm soil depth (quarterly in 2018). The water samples were immediately placed in a cooler and transported back to the lab where the samples were filtered and then tested for key nitrogen indicators in the ultraviolet and visible spectrophotometer (UV-7504, Xinmao Co. Ltd., Shanghai, China). The concentrations of NO_3^-–N, NO_2^-–N, and NH_4^+–N were analyzed by the zinc cadmium reduction method, naphthylethylenediamine photometric method, and hypobromite oxidation method, respectively; thus, DIN concentration was calculated as the sum of the values of NO_3^-–N, NO_2^-–N, and NH_4^+–N.

2.6. Statistical Analysis

We conducted statistical analyses using SPSS 11.0 (SPSS Inc., Chicago, IL, USA), and a significance level of $p < 0.05$ was used throughout. The scaling error (spatial variability) was defined as standard deviation of the GHG emissions measurements made on the same day (Lavoie et al., 2014; Richardson & Hollinger, 2005). The significant differences of GHG emissions and SGWP between the sites through time were assessed by a repeated measures ANOVA test. The significance between sample size and GHG fluxes variation in each month of the different wetland sites was analyzed by test of coefficient of variation. We used regression analyses to evaluate the influence of leaf chlorophyll concentration and light intensity on CO_2 emission fluxes, and the influence of soil ORP on CH_4 emission fluxes, which was judged statistically by the coefficient of determination, R^2, and its statistical significance was determined by one-way ANOVA.

3. Results

3.1. CO_2 Fluxes in the Restored and Natural Wetlands

The CO_2 fluxes represented daytime gross primary production with the negative value indicating CO_2 uptake and the positive value CO_2 release (Figure 1a). Overall, both the restored and natural wetlands showed clear seasonal patterns of CO_2 uptake during the growing season (Figure 1a).

In the restored wetland, while the plants were still dormant, the CO_2 uptake ability remained low. Especially in February, the average CO_2 flux values were positive (0.312 μmol m^{-2} s^{-1}), indicating a small CO_2 release from the wetland (Figure 1a). In March, plants displayed daytime CO_2 uptake (the CO_2 flux values were negative), then the uptake increased in spring, and maintained high values (40–47 μmol m^{-2} s^{-1}) in the

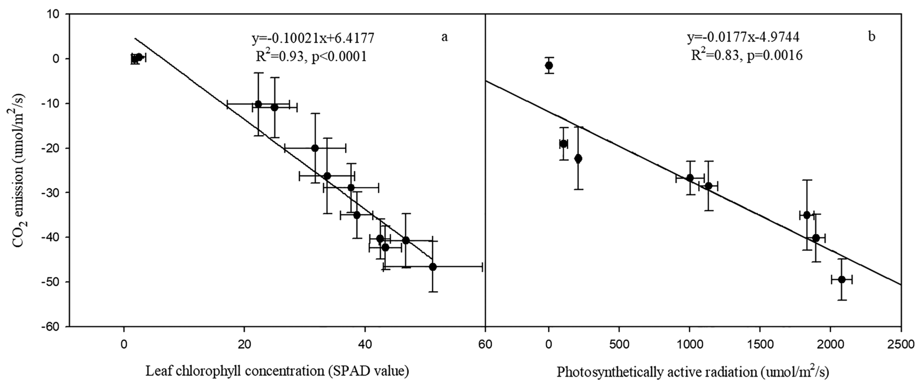

Figure 2. The linear relationships (a) between CO_2 emission fluxes and leaf chlorophyll concentration and (b) between CO_2 emission fluxes and the light intensity of the restored wetland.

summer coinciding with plant growth, which indicates the strong gross primary production of the wetland ecosystem. In the autumn, the plant photosynthetic capacity began to decrease and reached to a low level with plant senescing. There was a significant linear correlation between leaf chlorophyll concentration and CO_2 uptake ($R^2 = 0.93$, $p < 0.0001$; Figure 2a), which could explain the seasonal change of CO_2 uptake with the shifts of plant phenology. Since the correlation between CO_2 emission fluxes and leaf chlorophyll concentration in the natural wetland is similar to that in the restored wetland, we just plotted the correlation of the restored wetland. The CO_2 fluxes of natural wetland also showed seasonal change with the development of plants. However, the CO_2 uptake ability of natural wetland over the year (April–December) was significantly lower than that of restored wetland (Figure 1a; $p < 0.0001$, Table S2).

In addition, plant CO_2 uptake ability appeared to be influenced by daily changes in weather (sunny vs. cloudy). Diurnal measurements made on a midsummer day showed that plant CO_2 uptake was correlated with photosynthetically active radiation ($R^2 = 0.83$, $p = 0.0016$; Figures 2b and 3a). In the early morning and later afternoon, the plants showed low photosynthetic rate under low light intensity; plant CO_2 uptake ability became stronger with the increasing of light intensity and peaked (uptake 48 CO_2 μmol m^{-2} s^{-1}) at 14:00 with the greatest lighting. At night, plants ceased photosynthesis, and whole ecosystem dark respiration at 20:00 averaged 6.81 CO_2 μmol m^{-2} s^{-1}. We found that the CO_2 fluxes were relatively stable during 10:00–15:00, so subsequent campaigns were conducted during this midday time window.

3.2. CH_4 Emission in the Restored and Natural Wetlands

Generally, both the restored and natural wetlands represented CH_4 sources throughout the year. Compared with CO_2 flux, the CH_4 emission level of the wetlands was two order of magnitude lower.

In the restored wetland, before the active growing season began, CH_4 fluxes were very low (ranged from 0 to 0.05 μmol m^{-2} s^{-1}). In April, with rising temperature and plant growth, CH_4 flux increased; the peak of CH_4 emission reached 0.15 μmol m^{-2} s^{-1} in June. The CH_4 emission remained high in the summer and then reduced after entering the senescence stage (Figure 1b). There was no clear change of CH_4 emission during the day, which indicates that light intensity may not be the key environmental factor controlling CH_4 emission in the restored wetland (Figure 3b).

Comparatively, CH_4 emission fluxes of natural wetland were significantly higher than that of restored wetland ($p < 0.0001$, Table S2) and varied seasonally (increased with plants growth and decreased with plants aging). The CH_4 emission of the natural wetland peaked in August with the value of 0.48 μmol m^{-2} s^{-1}, which was four times higher than the maximum of restored wetland.

3.3. N_2O Emission in the Restored and Natural Wetlands

Similar to CH_4 fluxes, the N_2O emission values were positive, which revealed that the wetlands were N_2O sources. Figure 1c showed the seasonal patterns of N_2O fluxes in the restored and natural wetlands. In spring and winter, the uptake of N_2O within the restored wetland was minimal. Then, the N_2O fluxes increased substantially and peaked in June (N_2O fluxes were 0.07 and 0.06 μmol m^{-2} s^{-1} in the restored and

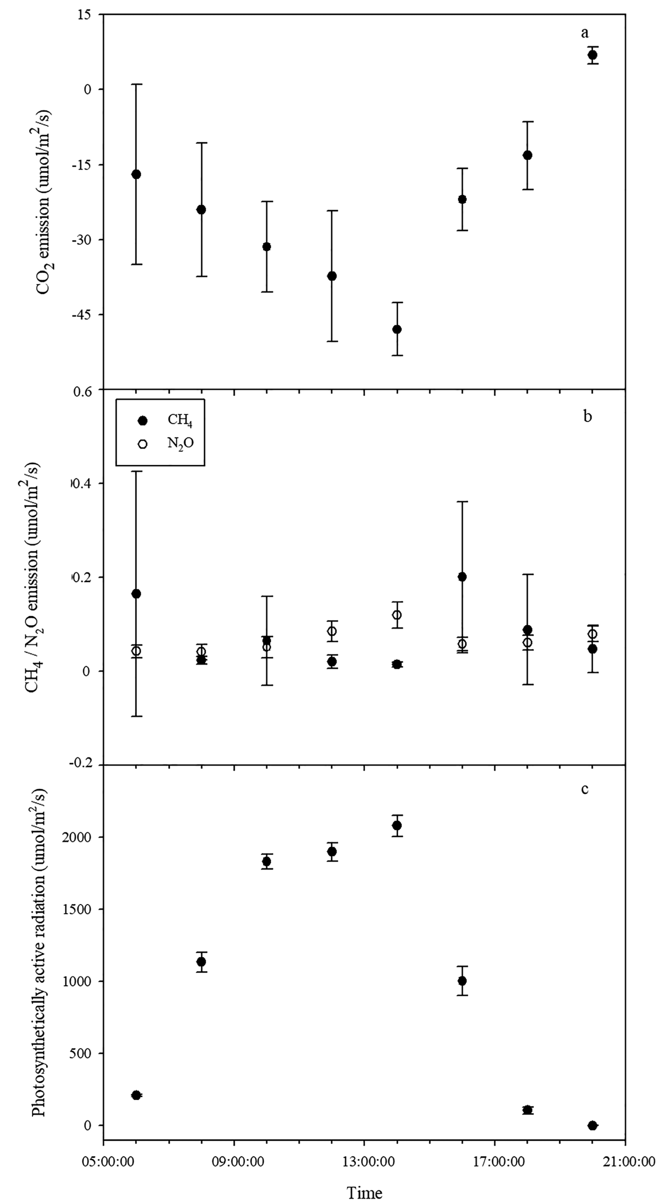

Figure 3. The diurnal variations of GHG emissions (mean ± SD) of the restored wetland on 15 July 2018.

natural wetlands, respectively). In late summer and autumn, the values dropped drastically, close to 0 in October. Similar to CH_4, N_2O flux had no notable correlation to photosynthetically active radiation in summer, with a range of 0.04–0.12 μmol m^{-2} s^{-1} (Figure 3c). There was no significant difference of the N_2O emission fluxes between the natural and restored wetlands ($p = 0.073$, Table S2).

3.4. The SGWP in the Restored and Natural Wetlands

Generally, the SGWP values of the restored and natural wetlands were negative, which indicated the wetlands could reduce the GHG emissions and potentially help to mitigate climate change progression. The lowest SGWP value appeared in May with the value of −0.065 kg CO_2 m^{-2} day $^{-1}$, which showed that the restored wetland had the strongest blue carbon potential at that time. In June, the SGWP of the restored wetland increased suddenly potentially due to the contribution of N_2O emission (Figures 1c and 4). Although the flux of N_2O was orders of magnitude lower than that of CO_2 and CH_4 (Figure 1), small changes of N_2O emission can shift the SGWP value of the wetland ecosystem.

Most notably, this study showed that the restored wetland had significantly lower SGWP compared to the natural wetland (Figure 4; $p <$ 0.0001, Table S2). The annual daytime SGWP value of the restored wetland was approximately 2.2 times that of the natural wetland (SGWP values were −11.23 and −5.04 kg CO_2 m^{-2} $year^{-1}$ from April to December in the restored and natural wetlands, respectively, Table 1), which indicates the restored wetland had a higher capability to mitigate climate change.

4. Discussion

4.1. GHG Fluxes in Restored and Natural Wetlands

In this study, greater CO_2 absorption of the restored wetlands relative to the natural wetlands was due to greater photosynthetic uptake by greater plants biomass (Windham et al., 2001). In the restored wetland, the plants grew well after transplantation, and the biomass was significantly higher ($p = 0.042$), leading to more CO_2 uptake in the restored wetland than that in the natural wetland, which reflected the success of the restoration plan (Table 1). This result is potentially due to the creation of a suitable microenvironment that facilitates rapid plant growth via "culvert valve control" in the restored wetland. After marsh establishment was completed, the eco-dike was opened to enable tidal access, thus further encouraging a self-sustaining wetland to promote ecosystem functions and services.

Meanwhile, we found that CO_2 uptake of restored wetland was significantly higher than natural wetland throughout the year, except in November (Figure 1a). During the dormant period (October and November), the spatial variation (i.e., standard deviation) across the plots were higher in both sites (Figure 1), indicating that there were "hotspots" and "hot moments" caused by unclear environmental factors in the non-growing season (He et al., 2010; Lavoie et al., 2014). Though our monthly measurements of the plots could represent the seasonal change of GHG emissions in the two sites (Table S3), the large flux uncertainty may affect evaluating the monthly integrated fluxes. Further work is needed to reduce the uncertainty in temporally integrated flux by increasing measurement frequency (He et al., 2010) or applying gap-filling algorithms when scaling estimates are derived from sporadic manual measurements in time as well as space (Gomez-Casanovas et al., 2013; Phillips et al., 2017; Richardson & Hollinger, 2005).

Additionally, the restored wetland emitted less CH_4 compared with the natural wetland, which may due to the ORP caused by different water managements (Table 1 and Figures 5 and 6). Mostly, the natural wetland

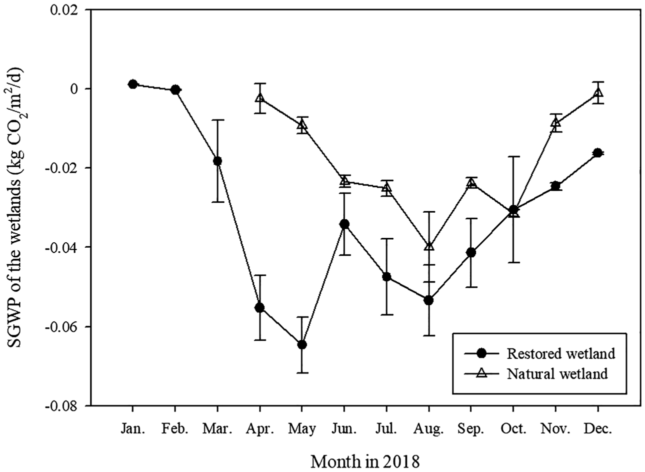

Figure 4. The seasonal variations of SGWP (mean ± SD) in the restored and natural wetlands. Here, the SGWP value represented the daytime carbon absorption capacity of the wetlands from 8 to 18 hr of a day.

did not undergo water exchange from low tide and consequently formed an anoxic condition and generated CH_4 (Figure 5). Therefore, in the restored wetland, we kept the water level at 10 cm and the flow rate at 0.03 m s^{-1} throughout the year. The manipulation of tidal flow can effectively reduce the CH_4 emission due to continuous water flow that disrupts the anoxic environment, thus inhibiting methanogenesis (Altor & Mitsch, 2006). Consequently, coastal ecosystems could switch from net sources to net sinks of carbon with efficient water exchange. Therefore, including tidal flow management in future wetland restoration/creation may be a feasible method for reducing CH_4 emission.

To determine the effect of water management on CH_4 emissions, we shut down the flow pump and evacuated the overlying water within the restored wetland for 2 weeks (13 August–28 August) to simulate the natural wetland under low tide. We found that continuous flow enhanced the ORP of water-soil interface, consequently decreasing CH_4 emission in the restored wetland (Figure 5).

Previous studies also stated that CH_4 emission was negatively related to wetland salinity (Chmura et al., 2011; Kroeger et al., 2017; Poffenbarger et al., 2011; Vivanco et al., 2015) because (1) sulfate-reducing bacteria outcompete methanogens for energy sources and then limiting CH_4 production (Poffenbarger et al., 2011; Weston et al., 2014) and (2) CH_4 oxidation by sulfate reducers can also inhibit CH_4 emission (Bartlett et al., 1987). However, our results showed that the natural wetland emitted higher CH_4, though it had a higher salinity level than the restored wetland (Table 1), which suggests that salinity is not the dominant factor influencing CH_4 emission in all moderate saline wetlands.

4.2. The Key Factors Affecting the Seasonal Dynamics of GHG Fluxes in Wetlands

Plant growth is important for carbon sequestration and preservation due to atmospheric CO_2 uptake from coastal wetland plants (Couto et al., 2014). There was a clear linkage between plant growth (leaf chlorophyll concentration) and daytime CO_2 uptake during the growing season, suggesting a strong role of vegetation photosynthesis in reducing GHG emission and enhancing C sequestration. Though *Phragmites australis* and *Spartina alterniflora* may have no significant difference in photosynthetic capacity with the similar leaf

Table 1
The Structural and Functional Properties of Blue Carbon in the Restored and Natural Wetlands

GHG fluxes and environmental variables	Restored wetland	Natural wetland
CO_2 emission (μmol m^{-2} s^{-1})	−43.22 ± 3.03	−36.75 ± 1.30
CH_4 emission (μmol m^{-2} s^{-1})	0.13 ± 0.02	0.43 ± 0.07
N_2O emission (μmol m^{-2} s^{-1})	0.05 ± 0.02	0.04 ± 0.02
SGWP (kg CO_2 m^{-2} $year^{-1}$)	−11.23 ± 4.34	−5.04 ± 3.73
pH	6.40 ± 0.13	6.45 ± 0.12
ORP (mV)	301.37 ± 52.77	203.33 ± 32.61
Soil moisture (%)	90.15 ± 5.84	82.93 ± 6.53
Water salinity (‰)	10.00 ± 1.22	19.28 ± 2.12
SOC content (%)	1.01 ± 0.08	0.93 ± 0.13
DIN concentration (mg L^{-1})	0.16 ± 0.01	0.18 ± 0.01
Plant composition	*Phragmites australis*	*Phragmites australis* (45%) and *Spartina alterniflora* (55%)
Plant biomass (kg m^{-2})	2.25 ± 0.19	2.04 ± 0.12
Water management	The water level was 10 cm, and the continuous flow rate was 0.03 m s^{-1}	Natural tide effect

Note. The SGWP value represented the annual sum (mean ± SD) calculated as daytime SGWP from 8 to 18 hr over 275 days (April–December), and other data represented the averaged values (mean ± SD) of the measurements during plants' maturation stage in the summer season (June–August).

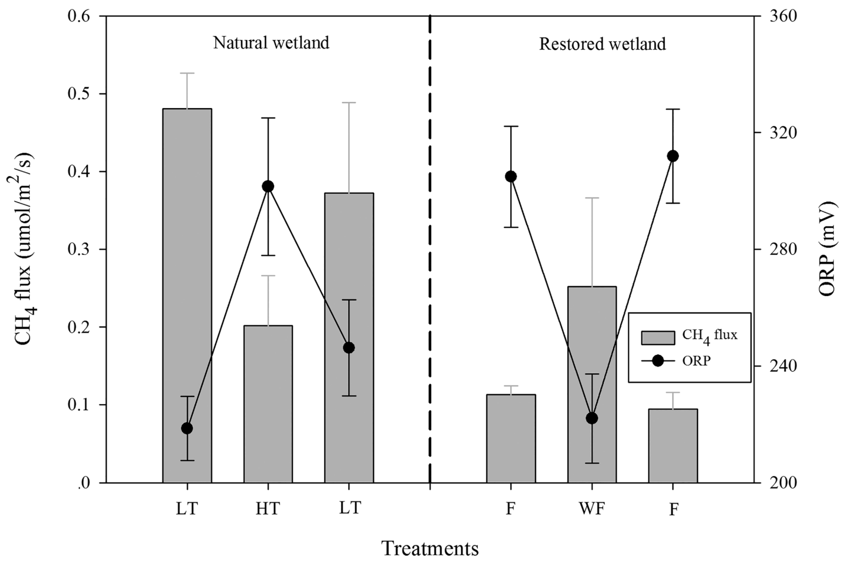

Figure 5. The CH_4 emissions and ORP of the restored and natural wetlands. In the natural wetland, measurements were taken on 3 July (low tide, LT), 13 July (high tide, HT), and 20 July (LT); in the restored wetland, measurements were taken on 10 August (flow rate of 0.03 m s^{-1}, F), 28 August (without flow, WF), and 5 September (flow rate of 0.03 m s^{-1}, F).

chlorophyll concentrations, Yingwuzhou wetland showed stronger carbon assimilation along with higher plant biomass than the natural wetland. However, despite the *Phragmites australis* biomass has a steady increase in its early establishment phase, the plant growth rate might decrease over years as the ecosystem further established in the future. CH_4 emission increased in the summer months, which is a similar pattern to plant growth as it increased during the same time period (Colmer, 2003; Koebsch et al., 2013). There are three main reasons that account for this phenomenon: (1) root respiration could accelerate O_2 consumption and anaerobic environment formation; (2) root exudates provide sufficient substrate for methanogens (Chidthaisong & Watanabe, 1997); and (3) plants' aerenchyma can also directly drive CH_4 transferring from soils to the atmosphere (Beckett et al., 2001; Colmer, 2003).

Temperature and light intensity are the important environmental drivers of GHG fluxes in wetlands. The seasonal change of daytime CO_2 uptake by wetland plants is mainly driven by temperature, photosynthetically active radiation, and day-length (Moseman-Valtierra et al., 2016). Previous studies reported that higher ambient temperature and light intensity could accelerate the activity of the primary C_4 photosynthetic enzyme (RuBisCO), resulting in higher CO_2 uptake (Abdul-Aziz et al., 2018; Guo et al., 2009; Inglett et al., 2012). Moreover, methanogenesis is substantially driven by temperature (Martin & Moseman-Valtierra, 2017), which could contribute to higher CH_4 emission during high temperatures. Walter and Heimann (2000) found that CH_4 production exponentially increased with elevated soil temperature, leading to higher CH_4 emissions. Similarly, the temperature variation may cause the seasonal change of N_2O fluxes. Higher temperatures would benefit the population growth and activity of nitrifiers and denitrifiers (Braker et al., 2010; Gamble et al., 1977), and consequently accelerate nitrification-denitrification processes and generate N_2O from wetland soils (Virdis et al., 2010).

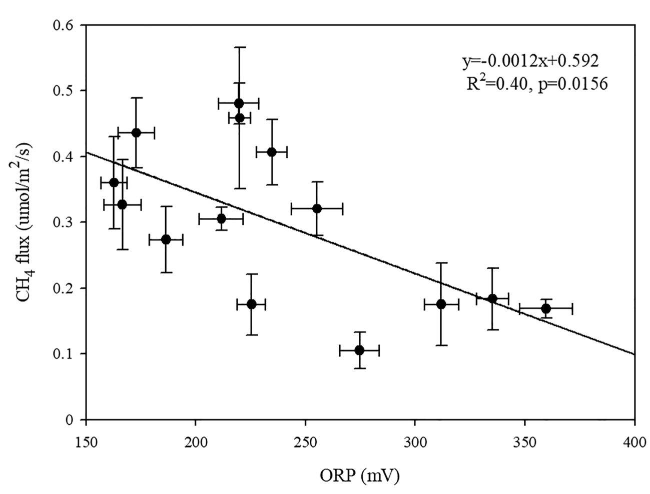

Figure 6. The linear regression demonstrating the influence of ORP on CH_4 emissions of the coastal wetlands in the summer season.

Our results showed that the restored wetland had relatively high N_2O emissions in the summer with high nitrogen loading. The DIN concentration of the pore water was 0.16 ± 0.01 mg L^{-1} in summer, which was twice higher than other seasons in the restored wetland (the DIN concentrations were 0.08 ± 0.01, 0.08 ± 0.02, and 0.09 ± 0.01 mg L^{-1} in spring, autumn, and winter, respectively). Previous studies (Gao et al., 2017; Lyu et al., 2017; Moseman-Valtierra et al., 2011) revealed that high nitrogen loading may lead to a considerable amount of N_2O emission from wetlands due to nitrification-denitrification processes, which is consistent with our result. Moreover, given the same DIN level in the pore water (Table 1) of the restored and natural wetlands, we suggested that the DIN level may not the main factor for the fast plant growth in our study.

4.3. The Evaluation and Comparison of Blue Carbon Capacity

The goal of our study was to analyze GHG emissions and blue carbon capacity of restored coastal wetlands and to support the need for blue carbon capacity to be an important restoration aim and evaluation index for wetland restoration on a global scale. As the results of this study demonstrate, a wetland's blue carbon capacity is an important factor when considering climate change progression, which has implications on human livelihood and development.

In general, the Yingwuzhou restored wetland emerged as a large carbon sink in 2018, and its annual daytime (8–18 hr) SGWP was -11.70 ± 7.77 kg CO_2 m^{-2} $year^{-1}$ (January–December, or -11.23 ± 4.34 kg CO_2 m^{-2} $year^{-1}$ if only accounting April to December; Table 1), which would be equivalent to 31.92 ± 21.20 MgC ha^{-1} $year^{-1}$ for daytime carbon sequestration. This rate exceeded the carbon sequestration rate of eutrophic impoundments at 21.2 MgC ha^{-1} $year^{-1}$ (Downing et al., 2008). Chmura et al. (2003) investigated 154 saline tidal wetlands and obtained a mean carbon sequestration rate of 1.4 MgC ha^{-1} $year^{-1}$, which is also considerably lower than the Yingwuzhou restored wetland because we only consider the daytime carbon uptake capacity in this study without accounting for nighttime respiratory loss of carbon. The ability of reducing GHG emissions was demonstrated more in the restored wetland than the natural wetland, which suggests that restoration of biological and physical conditions (e.g., species composition and water flow) could enhance carbon accumulation rates. These biological and physical conditions can be applied to future wetland restoration projects that occur in various geographical locations as a method to mitigate GHG emissions.

The principle restoration idea is to protect the site and help marsh establishment by engineering measures during the early phases of restoration, and thereafter, in the late phase, we will encourage the self-organization of the restored ecosystem. By proving the strong blue carbon capacity of the wetland restoration, we call for more worldwide implementations of this restoration engineering in degraded wetland areas. Badiou et al. (2011) compared the carbon sequestration potentials in newly (<5 years) restored and long-term (>5 years) restored wetlands in the Canadian prairies and found that the latter was 2.5 times than the former (with the unit as MgC ha^{-1} $year^{-1}$). This study only captured the second year following restoration and compared only a single pair of wetlands in a short-term study. Long-time monitoring of the interannual variability of GHG fluxes in more wetland sites is essential to predict GHG fluxes at longer timescales, which will improve the understanding of the feasibility and effectiveness of wetland restoration to enhance carbon sequestration. The results suggested that the restoration engineering of water flow rates was critical to carbon sequestration, which was substantiated by measurements of CH_4 emissions at different water levels. Hence, we plan to maintain the water level when the restoration process proceeds in the future. However, the long-term impacts of water level on SOC accumulation could not be determined from this short-duration study. It should be noted that GHG emissions from the wetlands themselves do not reflect the total amount of GHGs the wetland contributes to the ecosystem (Poffenbarger et al., 2011), since some fraction of the GHG produced may be transported in water outflow (e.g., DOC and DIC), which future studies should investigate.

5. Conclusion

This study broadened the knowledge of diurnal and seasonal variations of GHG (including CO_2, CH_4, and N_2O) emissions, as well as the key environmental factors impacting the vegetated restored wetland. Our experiment revealed that water regulation and adequate plant biomass is emerging as an effective method to promote carbon storage in restored coastal habitats. Our study also quantified a new and previously undervalued strategy for mitigating climate change that maximizes CO_2 uptake and minimizes CH_4 emissions in restored wetlands. The methods that have shown effective in this study can be applied to wetland restoration projects in other geographical locations as a mechanism to maintain salt marshes as carbon sinks and help mitigate GHG emissions.

Acknowledgments

We would like to thank Yangtze Delta Estuarine Wetland Ecosystem Ministry of Education & Shanghai Observation and Research Station for providing sites during our research. This research was supported by the National Key Research and Development Program of China (Grant 2017YFC0506002), the National Natural Science Foundation of China Overseas and Hong Kong-Macao Scholars Collaborative Research Fund (Grant 31728003), the China Postdoctoral Science Foundation (Grant 2018M640362), the Shanghai University Distinguished Professor (Oriental Scholars) Program (Grant JZ2016006), the Open Fund of Shanghai Key Lab for Urban Ecological Processes and Eco-Restoration (Grant SHUES2018B06), and the Scientific Projects of Shanghai Municipal Oceanic Bureau (Grant 2018-03). The complete data set is available at https://data.4tu.nl/repository/uuid:536b2614-c4ca-43d2-84dd-6180fd859544.

References

Abdul-Aziz, O. I., Ishtiaq, K. S., Tang, J., Moseman-Valtierra, S., Kroeger, K. D., Gonneea, M. E., et al. (2018). Environmental controls, emergent scaling, and predictions of greenhouse gas (GHG) fluxes in coastal salt marshes. *Journal of Geophysical Research: Biogeosciences*, *123*, 2234–2256. https://doi.org/10.1029/2018JG004556

Altor, A. E., & Mitsch, W. J. (2006). Methane flux from created riparian marshes: Relationship to intermittent versus continuous inundation and emergent macrophytes. *Ecological Engineering*, *28*, 224–234. https://doi.org/10.1016/j.ecoleng.2006.06.006

Badiou, P., McDougal, R., Pennock, D., & Clark, B. (2011). Greenhouse gas emissions and carbon sequestration potential in restored wetlands of the Canadian prairie pothole region. *Wetlands Ecology and Management*, *19*, 237–256. https://doi.org/10.1007/s11273-011-9214-6

Bartlett, K. B., Bartlett, D. S., Harriss, R. C., & Sebacher, D. I. (1987). Methane emissions along a salt marsh salinity gradient. *Biogeochemistry*, *4*(3), 183–202. https://doi.org/10.2307/1468663

Beckett, P. M., Armstrong, W., & Armstrong, J. (2001). Mathematical modelling of methane transport by *Phragmites*: The potential for diffusion within the roots and rhizosphere. *Aquatic Botany*, *69*, 293–312. https://doi.org/10.1016/s0304-3770(01)00144-9

Boucher, O., & Haywood, J. (2001). On summing the components of radiative forcing of climate change. *Climate Dynamics*, *18*(3-4), 297–302. https://doi.org/10.1007/s003820100185

Braker, G., Schwarz, J., & Conrad, R. (2010). Influence of temperature on the composition and activity of denitrifying soil communities. *FEMS Microbiology Ecology*, *73*(1), 134–148. https://doi.org/10.1111/j.1574-6941.2010.00884.x

Brannon, E. Q., Moseman-Valtierra, S. M., Rella, C. W., Martin, R. M., Chen, X. C., & Tang, J. W. (2016). Evaluation of laser-based spectrometers for greenhouse gas flux measurements in coastal marshes. *Limnology and Oceanography: Methods*, *14*(7), 466–476. https://doi.org/10.1002/lom3.10105

Chidthaisong, A., & Watanabe, I. (1997). Methane formation and emission from flooded rice soil incorporated with ^{13}C labelled rice straw. *Soil Biology and Biochemistry*, *29*, 1173–1181. https://doi.org/10.1016/S0038-0717(97)00034-5

Chmura, G. L., Anisfeld, S. C., Cahoon, D. R., & Lynch, J. C. (2003). Global carbon sequestration in tidal, saline wetland soils. *Global Biogeochemical Cycles*, *17*(4), 1–12. https://doi.org/10.1029/2002gb001917

Chmura, G. L., Kellman, L., & Guntenspergen, G. R. (2011). The greenhouse gas flux and potential global warming feedbacks of a northern macrotidal and microtidal salt marsh. *Environmental Research Letters*, *6*(4), 044016. https://doi.org/10.1088/1748-9326/6/4/044016

Colmer, T. D. (2003). Long-distance transport of gases in plants: A perspective on internal aeration and radial oxygen loss from roots. *Plant, Cell and Environment.*, *26*, 17–36. https://doi.org/10.1046/j.1365-3040.2003.00846.x

Couto, T., Duarte, B., Martins, I., Cacador, I., & Marques, J. C. (2014). Modelling the effects of global temperature increase on the growth of salt marsh plants. *Applied Ecology and Environmental Research*, *12*(3), 753–764. https://doi.org/10.15666/aeer/1203_753764

Downing, J. A., Cole, J. J., Middelburg, J. J., Striegl, R. G., Duarte, C. M., Kortelainen, P., et al. (2008). Sediment organic carbon burial in agriculturally eutrophic impoundments over the last century. *Global Biogeochemical Cycles*, *22*(1). https://doi.org/10.1029/2006GB002854

Frolking, S., Roulet, N., & Fuglestvedt, J. (2006). How northern peatlands influence the Earth's radiative budget: Sustained methane emission versus sustained carbon sequestration. *Journal of Geophysical Research*, *111*, G01008. https://doi.org/10.1029/2005JG000091

Gamble, T. N., Betlach, M. R., & Tiedje, J. M. (1977). Numerically dominant denitrifying bacteria from world soils. *Applied and Environmental Microbiology*, *33*, 926–939. https://aem.asm.org/content/aem/33/4/926.full.pdf

Gao, L., Zhou, W., Huang, J., He, S., Yan, Y., Zhu, W., et al. (2017). Nitrogen removal by the enhanced floating treatment wetlands from the secondary effluent. *Bioresource Technology*, *234*, 243–252. https://doi.org/10.1016/j.biortech.2017.03.036

García-Lledó, A., Vilar-Sanz, A., Trias, R., Hallin, S., & Bañeras, L. (2011). Genetic potential for N_2O emissions from the sediment of a free water surface constructed wetland. *Water Research*, *45*(17), 5621–5632. https://doi.org/10.1016/j.watres.2011.08.025

Gomez-Casanovas, N., Anderson-Teixeira, K., Zeri, M., Bernacchi, C. J., & DeLucia, E. H. (2013). Gap filling strategies and error in estimating annual soil respiration. *Global Change Biology*, *19*, 1941–1952. https://doi.org/10.1111/gcb.12127

Guo, H., Noormets, A., Zhao, B., Chen, J., Sun, G., Gu, Y., et al. (2009). Tidal effects on net ecosystem exchange of carbon in an estuarine wetland. *Agricultural and Forest Meteorology*, *149*(11), 1820–1828. https://doi.org/10.1016/j.agrformet.2009.06.010

He, H., Liu, M., Sun, X., Zhang, L., Luo, Y., Wang, H., et al. (2010). Uncertainty analysis of eddy flux measurements in typical ecosystems of ChinaFLUX. *Ecological Informatics*, *5*, 492–502. https://doi.org/10.1016/j.ecoinf.2010.07.004

Inglett, K. S., Reddy, K. R., & Osborne, T. Z. (2012). Temperature sensitivity of greenhouse gas production in wetland soils of different vegetation. *Biogeochemistry*, *108*(1–3), 77–90. https://doi.org/10.1007/s10533-011-9573-3

Intergovernmental Panel on Climate Change (2014). Core Writing Team, R. K. Pachauri, & L. A. Meyer (Eds.), Climate change 2014: Synthesis report. Contribution of Working Groups I, II and III to the Fifth Assessment Report of the Intergovernmental Panel on Climate Change (pp. 151). Geneva, Switzerland: IPCC.

Jain, A. K., Briegleb, B. P., Minschwaner, K. M., & Wuebbles, D. J. (2000). Radiative forcings and global warming potentials of 39 greenhouse gases. *Journal of Geophysical Research*, *105*, 20,773–20,790. https://doi.org/10.1029/2000JD900241

Kirwan, M. L., & Megonigal, J. P. (2013). Tidal wetland stability in the face of human impacts and sea-level rise. *Nature*, *504*(7478), 53–60. https://doi.org/10.1038/nature12856

Kirwan, M. L., Temmerman, S., Skeehan, E. E., Guntenspergen, G. R., & Fagherazzi, S. (2016). Overestimation of marsh vulnerability to sea level rise. *Nature Climate Change*, *6*(3), 253–260. https://doi.org/10.1038/nclimate2909

Koebsch, F., Glatzel, S., & Jurasinski, G. (2013). Vegetation controls methane emissions in a coastal brackish fen. *Wetlands Ecology and Management*, *21*(5), 323–337. https://doi.org/10.1007/s11273-013-9304-8

Kroeger, K. D., Crooks, S., Moseman-Valtierra, S., & Tang, J. W. (2017). Restoring tides to reduce methane emissions in impounded wetlands: A new and potent Blue Carbon climate change intervention. *Scientific Reports*, *7*(1), 11914. https://doi.org/10.1038/s41598-017-12138-4

Lavoie, M., Phillips, C. L., & Risk, D. (2014). A practical approach for uncertainty quantification of high frequency soil respiration using Forced Diffusion chambers. *Journal of Geophysical Research: Biogeosciences*, *120*, 128–146. https://doi.org/10.1002/2014JG002773

Lyu, W., Huang, L., Xiao, G., & Chen, Y. (2017). Effects of carbon sources and COD/N ratio on N_2O emissions in subsurface flow constructed wetlands. *Bioresource Technology*, *245*(Pt A), 171–181. https://doi.org/10.1016/j.biortech.2017.08.056

Mander, Ü., Maddison, M., Soosaar, K., Koger, H., Teemusk, A., Truu, J., et al. (2015). The impact of a pulsing water table on wastewater purification and greenhouse gas emission in a horizontal subsurface flow constructed wetland. *Ecological Engineering*, *80*, 69–78. https://doi.org/10.1016/j.ecoleng.2014.09.075

Martin, R. M., & Moseman-Valtierra, S. (2017). Different short-term responses of greenhouse gas fluxes from salt marsh mesocosms to simulated global change drivers. *Hydrobiologia*, *802*(1), 71–83. https://doi.org/10.1007/s10750-017-3240-1

Mcleod, E., Chmura, G. L., Bouillon, S., Salm, R., Björk, M., Duarte, C. M., et al. (2011). A blueprint for blue carbon: Toward an improved understanding of the role of vegetated coastal habitats in sequestering CO_2. *Frontiers in Ecology and the Environment*, *9*, 552–560. https://doi.org/10.1890/110004

Mitsch, W. J., & Gosselink, J. G. (2000). *Wetlands* (p. 295). New York: NY USA.

Moseman-Valtierra, S., Abdul-Aziz, O. I., Tang, J., Ishtiaq, K. S., Morkeski, K., Mora, J., et al. (2016). Carbon dioxide fluxes reflect plant zonation and belowground biomass in a coastal marsh. *Ecosphere*, *7*, e01560. https://doi.org/10.1002/ecs2.1560

Moseman-Valtierra, S., Gonzalez, R., Kroeger, K. D., Tang, J. W., Chao, W. C., Crusius, J., et al. (2011). Short-term nitrogen additions can shift a coastal wetland from a sink to a source of N_2O. *Atmospheric Environment*, *45*(26), 4390–4397. https://doi.org/10.1016/j.atmosenv.2011.05.046

National Academy of Sciences (2018). *Negative emissions technologies and reliable sequestration: A research agenda* (p. 356). Washington DC: The National Academies Press.

Neubauer, S. C., & Megonigal, J. P. (2015). Moving beyond global warming potentials to quantify the climatic role of ecosystems. *Ecosystems*, *18*(6), 1000–1013. https://doi.org/10.1007/s10021-015-9879-4

Phillips, C. L., Bond-Lamberty, B., Desai, A. R., Lavoie, M., Risk, D., Tang, J., et al. (2017). The value of soil respiration measurements for interpreting and modeling terrestrial carbon cycling. *Plant Soil*, *413*(1-2), 1–25. https://doi.org/10.1007/s11104-016-3084-x

Poffenbarger, H. J., Needelman, B. A., & Megonigal, J. P. (2011). Salinity influence on methane emissions from tidal marshes. *Wetlands*, *31*(5), 831–842. https://doi.org/10.1007/s13157-011-0197-0

Richardson, A., & Hollinger, D. Y. (2005). Statistical modeling of ecosystem respiration using eddy covariance data: Maximum likelihood parameter estimation, and Monte Carlo simulation of model and parameter uncertainty, applied to three simple models. *Agricultural and Forest Meteorology*, *131*, 191–208. https://doi.org/10.1016lj.agrfomet.2005.05.008

Rosentreter, J. A., Maher, D. T., Erler, D. V., Murray, R. H., & Eyre, B. D. (2018). Methane emissions partially offset "blue carbon" burial in mangroves. *Science Advances*, *4*(6), eaao4985. https://doi.org/10.1126/sciadv.aao4985

Tang, J., Ye, S., Chen, X., Yang, H., Sun, X., Wang, F., et al. (2018). Coastal blue carbon: Concept, study method, and the application to ecological restoration. *Science China Earth Sciences*, *61*(6), 637–646. https://doi.org/10.1007/s11430-017-9181-x

Virdis, B., Rabaey, K., Rozendal, R. A., Yuan, Z., & Keller, J. (2010). Simultaneous nitrification, denitrification and carbon removal in microbial fuel cells. *Water Research*, *44*(9), 2970–2980. https://doi.org/10.1016/j.watres.2010.02.022

Vivanco, L., Irvine, I. C., & Martiny, J. B. (2015). Nonlinear responses in salt marsh functioning to increased nitrogen addition. *Ecology*, *96*(4), 936–947. https://doi.org/10.1890/13-1983.1

Vuong, T. X., Heitkamp, F., Jungkunst, H. F., Reimer, A., & Gerold, G. (2013). Simultaneous measurement of soil organic and inorganic carbon: evaluation of a thermal gradient analysis. *Journal of Soils and Sediments*, *13*(7), 1133–1140. https://doi.org/10.1007/s11368-013-0715-1

Walter, B. P., & Heimann, M. (2000). A process-based, climate-sensitive model to derive methane emissions from natural wetlands: Application to five wetland sites, sensitivity to model parameters, and climate. *Global Biogeochemical Cycles*, *14*, 745–765. https://doi.org/10.1029/1999GB001204

Weston, N. B., Neubauer, S. C., Velinsky, D. J., & Vile, M. A. (2014). Net ecosystem carbon exchange and the greenhouse gas balance of tidal marshes along an estuarine salinity gradient. *Biogeochemistry*, *120*, 163–189. https://doi.org/10.1007/s10533-014-9989-7

Windham, L., Weis, J. S., & Weis, P. (2001). Patterns and processes of mercury release from leaves of two dominant salt marsh macrophytes, *Phragmites australis* and *Spartina alterniflora*. *Estuaries*, *24*, 787–795. https://doi.org/10.2307/1353170

Yang, H., Yang, X., Heskel, M., Sun, S., & Tang, J. (2017). Seasonal variations of leaf and canopy properties tracked by ground-based NDVI imagery in a temperate forest. *Scientific Reports*, *7*(1), 1267. https://doi.org/10.1038/s41598-017-01260-y

Zhou, C. H., Mao, Q. Y., Xu, X., Fang, C. M., & Luo, Y. M. (2016). Preliminary analysis of C sequestration potential of blue carbon ecosystems on Chinese coastal zone. *Scientia Sinica Vitae*, *46*(4), 475–486. https://doi.org/10.1360/N052016-00105

Erratum

In the originally published version of this article, Equation 2 ($SGWP = FCO_2 + 45FCH_4 + 270FN_2O$), FCO_2, FCH_4, FN_2O erroneously published as molar flux in units (e.g., μmol CO_2 m^{-2} s^{-1}). As a result, Table 1, Figure 4, and Table S2 published incorrectly. Although calculation results were incorrect using this equation, the conclusion of the paper was not influenced.

Corrections were made on the following pages:

Page 1. Abstract: "-10.32 ± 4.29" changed to "-11.23 ± 4.34"
Page 1. Abstract: "-0.76 ± 3.07" changed to "-5.04 ± 3.73"
Page 3. Under Equation (2): "where FCO_2, FCH_4, FN_2O are mass flux in units
(for example, μgCO_2 m^{-2} s^{-1})" added
Page 6. "-0.064" changed to "-0.065"
Page 6. "13" to "2.2" "-10.32 and -0.76" changed to "-11.23 and -5.04"
The article text, Figure 4, Table 1, and Table S2 have since been corrected, and this version may be considered the authoritative version of record.